A Peptide-Based Dendrimer That Enhances the Splice-Redirecting Activity of PNA Conjugates in Cells

Fatouma Said Hassane,[†] Gabriela D. Ivanova,[‡] Eleonora Bolewska-Pedyczak,[§] Rachida Abes,[†] Andrey A. Arzumanov,[‡] Michael J. Gait,[‡] Bernard Lebleu,[†] and Jean Gariépy*,[§]

UMR 5235 CNRS, Université Montpellier 2, Place Eugene Bataillon, 34095 Montpellier, France, Medical Research Council, Laboratory of Molecular Biology, Hills Road, Cambridge CB2 0QH, United Kingdom, and Department of Medical Biophysics, University of Toronto, 610 University Avenue, Toronto, M5G 2M9, Ontario, Canada. Received February 16, 2009; Revised Manuscript Received June 1, 2009

The full therapeutic potential of oligonucleotide (ON)-based agents has been hampered by cellular delivery challenges. Cell-penetrating peptides (CPP) represent promising delivery vectors for nucleic acids, and their potential has recently been evaluated using a functional splicing redirection assay, which capitalizes on the nuclear delivery of splice-correcting steric-block ON analogues such as peptide nucleic acids (PNA). Despite encouraging in vitro and in vivo data with arginine-rich CPP-steric block conjugates, mechanistic studies have shown that entrapment within the endosome/lysosome compartment after endocytosis remains a limiting factor. Previous work from our group has shown that CPP oligomerization greatly improves cellular delivery and increases transfection of plasmid DNA. We now report the chemical synthesis and the evaluation of multivalent CPP–PNA constructs incorporating monomeric (p53^{mono}) and dendrimer-like tetrameric (p53^{tet}) forms of the p53 tetramerization domain containing peptide, a 10 arginine CPP domain (R10), and a splice redirecting PNA (PNA705). These CPP–PNA conjugates were termed R10p53^{tet}-PNA705 and R10p53^{mono}-PNA705, referring to their oligomerization state. The present study demonstrates that the splicing redirection efficiency of PNA705 is much greater in the context of the tetrameric R10p53^{tet}-PNA705 construct than for the monomeric and occurs at nanomolar concentrations, demonstrating that multivalency is an important factor in delivering PNA into cells.

INTRODUCTION

Oligonucleotide (ON)-based agents have shown great potential in regulating gene expression and are routinely used to carry out functional genomics analyses. However, neither natural nucleic acids nor their chemically modified homologues are taken up efficiently by most cell types. While this challenge is easily circumvented through the use of transfection techniques in cultured cells, the systemic delivery of ONs in experimental animals remains a major limitation. Likewise, clinical trials with antisense ONs have resulted in mixed successes (*1*). Even very potent agents such as siRNAs have led to few clinical trials so far, due to a lack of efficient and nontoxic delivery vectors. Cell-penetrating peptides (CPP) represent good candidates for the intracellular delivery of nucleic acids with short oligoarginine motifs and peptides derived from the HIV Tat protein (Tat 48−60) and the Antennapedia homeodomain (Penetratin) being the most widely cited CPPs. The evaluation of CPPs in delivering functional ONs can best be achieved using the splicing redirection assay proposed by Kole (*2*). The assay is based on the splicing alteration in the β-globin gene in thalassemia. Intronic mutations (such as mutation 705 in intron 2) activate cryptic splice sites in this gene leading to a nonfunctional mRNA. This mutated intron has been introduced into the coding region of a reporter luciferase gene, and the construct has been stably transfected into HeLa cells. Masking the 705 mutated site with an antisense ON results in the reorientation of the splicing machinery toward intron elimination

and to luciferase expression. The assay is easy to implement (assessing splicing by luminescence or by RT-PCR) and provides signals covering a high dynamic range. It has now been adopted by many groups in the field of drug delivery as a convenient way to compare the performance of various CPP carriers in delivering ON analogues (*3−6*). A broad range of ON analogues has been synthesized to date that do not recruit RNase H. However, peptide nucleic acids (PNA) and phosphorodiamidate morpholino oligomer (PMO) analogues are particularly suited as therapeutic agents since they are RNase H incompetent, are metabolically stable, and hybridize to RNA with high affinity and specificity. Initial assays with a panel of CPPs including Tat 48−60, Penetratin, oligo-Arg, or oligo-Lys have been disappointing, since no efficient splicing correction could be demonstrated in the absence of endosomolytic agents at submicromolar CPP−ON conjugate concentrations. By contrast, encouraging data have been obtained with an arginine-rich peptide named (RXR)$_4$-PNA or -PMO (where X stands for an unnatural aminohexanoyl moiety) (*7*), with R$_6$-Penetratin-PNA (in which an Arg-rich tail has been appended to Penetratin) (*8*), and with the subsequent serum-stable Pip-PNAs (*9*). Dose-dependent and sequence-specific splicing correction has been achieved at micromolar or slightly lower concentrations in the absence of endosomolytic agents. Importantly, these PMO and PNA conjugates of Arg-rich CPPs also lead to splicing redirection in murine models of Duchenne muscular dystrophy (DMD) (*10, 11*). Such peptides are being evaluated for clinical applications, such as DMD, but it remains unclear at present whether the CPP-PMO doses required to be administered to humans will avoid potential liver and other toxic effects.

As far as mechanisms are concerned, it is now generally considered that CPP-PNA and PMO conjugates are taken up by endocytosis after binding to cell surface heparan sulfates.

---

* Corresponding author. Jean Gariepy, Ph.D., professor, Tel: 416-946-2967; fax: 416-946-6529; E-mail: gariepy@uhnres.utoronto.ca.
† UMR 5235 CNRS.
‡ Medical Research Council, Laboratory of Molecular Biology.
§ University of Toronto.

Structure activity (SAR) and mechanistic studies currently in progress with conjugates based on both $(RXR)_4$ and Pip CPP types have confirmed that entrapment within endocytic vesicles remains a major limitation. Studies of $(RXR)_4$-PMO intracellular distribution, in particular, clearly demonstrated that splicing redirection activity was due to the low amount of material that escaped from entrapment within endocytic vesicles.

The multivalent display of peptides harboring arginine- or lysine-containing CPP import sequences has been shown to dramatically enhance the cellular uptake levels of associated cargoes (*12, 13*). Specifically, synthetic branched peptides incorporating CPP sequences (loligomers) (*12, 14, 15*) as well as recombinant peptide constructs containing a self-assembling motif such as the p53 tetramerization domain (*13, 16*) have been shown to carry more efficiently drugs and chromophores into cells than the equivalent concentration of monomeric CPP homologues (*15*). Similarly, the condensation of such multivalent CPP dendrimers with plasmids results in particle complexes displaying excellent efficiency in entering targeted cells (*14*). In this report, we discuss the chemical assembly and evaluation of multivalent CPP−PNA constructs incorporating monomeric and tetrameric forms of a p53^{tet} domain containing peptide (p53^{tet}), a 10 arginine CPP domain (R10), and a splice redirecting PNA (PNA705). These CPP−PNA conjugates were termed R10p53^{tet}-PNA705 and R10p53^{mono}-PNA705 constructs, referring to their oligomerization state. The present study demonstrates that multivalency is an important factor in delivering PNA into cells.

EXPERIMENTAL PROCEDURES

Synthesis of PNA. The N-terminal nitropyridyl (Npys) cysteine-containing PNA705 (NH$_2$-Cys(NPys)-Lys-CCTCT-TACCTCAGTTACA-Lys-amide) was synthesized on a Liberty microwave peptide synthesizer (CEM) by the Fmoc/Bhoc solid-phase method as previously described using monomers obtained from Link Technologies Ltd. (Lanarkshire, Scotland) or Panagene Inc. (Daejeon, Korea), purified by HPLC, and analyzed by MALDI-TOF mass spectrometry on a Voyager DE Pro BioSpectrometry workstation as previously described (*9, 17*).

Synthesis and Characterization of R10p53 Peptides. The peptides R10p53^{tet} (R$_{10}$GEYFTLQIRGRERFEMFRELNEALE-LKDAQAGCGH$_6$) and R10p53^{mono} (R$_{10}$GEYFTLQIRGRERF-EMFRE$\underline{P}$NEALELKDAQAGCGH$_6$) were assembled by Fmoc solid-phase peptide synthesis as previously described (*16*). A single mutation of Leucine 344 to Proline (underlined residue) prevents tetramerization. A single cysteine residue was also introduced at their C-terminal end for the subsequent directional coupling of PNA. Peptides were purified to homogeneity by reverse-phase HPLC, and their sequences were confirmed by MALDI-TOF masses: R10p53^{tet}, calculated 6363.3, found 6361.2; R10p53^{mono}, calculated 6347.2, found 6345.2. The oligomerization status of R10p53 peptides was confirmed by cross-linking these peptides with glutaraldehyde followed by SDS-PAGE, which reveals the presence of a distinctive ladder of protein bands (monomer, dimer, and oligomers of p53 peptides) in the case of tetrameric p53^{tet}-containing peptides (Figure 1) as described elsewhere (*18*).

Peptide−PNA Conjugates. Single cysteine residues were inserted in both PNA 705 and R10p53 peptides to covalently link peptide and PNA via a disulfide bond (Table 1) as previously described, using a 2.5-fold excess of peptide component over NPys PNA component. Conjugate purifications were carried out by reverse-phase HPLC and analyzed by MALDI-TOF mass spectrometry as described elsewhere (*9, 17*). MALDI-TOF masses: R10p53^{tet}-PNA705, calculated 11487.3, found 11485.4; R10p53^{mono}, calculated 11471.3, found 11467.0.

Cells and Cell Culture. HeLa pLuc705 cells were stably transfected with pLuc/705 plasmid in which the coding sequence
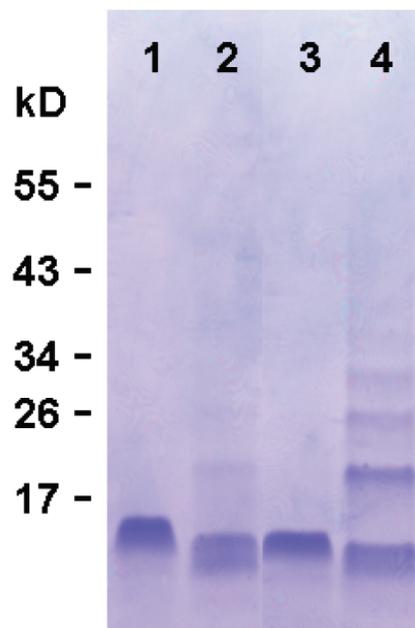
Figure 1. Glutaraldehyde cross-linking of monomeric and tetrametic p53 peptides demonstrating the presence of R10p53 peptide oligomers only for the tetrameric R10p53^{tet} peptide. Coomassie-stained SDS PAGE gel highlights a single protein band migration pattern for unmodified monomeric R10p53 peptide analogue (harboring a L344P mutation; lane 1, p53^{mono}) or cross-linked with 0.2% glutharaldehyde for 20 min (lane 2). The unmodified form of the tetrameric R10p53 analogue (lane 3) generates a comparable single band pattern, while the presence of glutaraldehyde results in a characteristic ladder of protein bands associated with the presence of R10p53^{tet} domain oligomers in solution.

Table 1. Sequences of PNA Conjugates

	S ▬▬ S	
p53 peptide	GCGH$_6$	CK-PNA705-K

p53^{mono}=R$_{10}$GEYFTLQIRGRERFEMFRE$\underline{L}$NEALELKDAQA

p53^{tet}=R$_{10}$GEYFTLQIRGRERFEMFRE$\underline{P}$NEALELKDAQA

PNA 705=cctcttacctcagttaca

of the luciferase gene is interrupted by the mutated intron 2 of the human β globin gene. Cells were cultured at 37 °C, 5% CO$_2$, as exponentially growing subconfluent monolayers in DMEM medium (Gibco, Cergy-Pontoise, France) supplemented with 10% fetal bovine serum (FBS).

Splicing Redirection Assay. The PNA conjugates incorporating either monomeric or tetrameric R10p53 or $(RXR)_4$ were incubated for 1 h at 37 °C in 1 mL optiMEM with exponentially growing HeLa pLuc 705 cells (1.75×10^5 cells/well seeded and cultivated overnight in 24 well plates). Cells were then washed twice with ice-cold PBS and incubation continued for 23 h in complete DMEM supplemented with 10% FBS. Cells were washed twice with ice-cold PBS and lysed with Reporter Lysis Buffer (Promega, Madison, WI, USA). The same protocol was used for HeLa pLuc 705 cells treated with 100 μM chloroquine (Figure 4B). Luciferase activity was measured using a Berthold Centro LB 960 luminometer (Berthold Technologies, Bad Wildbad, Germany) using the Luciferase Assay System substrate (Promega, Madison, WI, USA). Cellular protein concentrations were measured with the BCAProtein Assay Kit (Pierce, Rockford, IL, USA) and read using an ELISA plate reader (Dynatech MR 5000, Dynatech Laboratories, Chantilly,

VA, USA) at 550 nm. Luciferase activities were expressed as relative luminescence units (RLU) per μg protein. All experiments were performed in triplicate. Each data point represents the average of three replicates.

RT-PCR Analysis of Splicing Redirection. Total RNA was extracted from cellular lysates obtained as described in the previous paragraph using the Tri-Reagent kit (Sigma, St. Quentin Fallavier, France) according to manufacturer's instructions. The extracted RNA was amplified by RT-PCR (MJ Research PTC 200 Peltier Thermal Cycler) with forward primer 5′TTG ATA TGT GGA TTT CGA GTC GTC3′ and reverse primer 5′TGT CAA TCA GAG TGC TTT TGG CG3′. The products were analyzed by electrophoresis on a 2% agarose gel.

Saponin Cell Permeabilization. Exponentially growing HeLa pLuc705 cells (1.75×10^5 cells seeded and grown overnight in 24 well plates) were coincubated with the PNA conjugate and with 20 μg/mL of saponin for 30 min. The cells were then washed and incubation continued for 24 h in complete medium (DMEM plus 10% FBS). Cells were washed twice with ice-cold PBS, lysed with reporter lysis buffer, and processed as described above.

RESULTS

Design and Characterization of p53^{tet} Domain-Based PNA Delivery Peptides. As described in the Introduction, the human p53^{tet} tetramerization domain (residues 325−355; GEY-FTLQIRGRERFEMFRELNEALELKDAQA) is able to self-assemble into a well-defined tetramer in solution and to enhance the cellular import of conjugated cationic CPPs, as compared to its monomeric counterpart (*13, 16*). Importantly, the condensation of NLS-R10-p53^{tet} with luciferase reporter plasmid DNA led to complexes that increased the levels of luciferase expression in cells when compared to p53^{mono} constructs (*16*). In terms of designing CPP vectors better able to deliver steric-block ON analogues into cells, we have synthesized a new CPP construct in which an arginine-rich motif (R10) has been attached to the tetramerization domain (residues 325−355) of the human p53 protein. A cysteine was inserted near its C-terminus to covalently attach a PNA, while a short His$_6$ tag was added for purification purposes (Table 1).

The synthetic peptide was chemically conjugated to a splice-redirecting 18-base-long PNA complementary to the 705 splice site (PNA 705), which we have used extensively in conjugation with other CPPs (*9*). In contrast to our previous CPP-p53^{tet} conjugates designed for plasmid delivery, no nuclear localization signal was included in the construct, since the molecular mass of the conjugate should be small enough to allow diffusion from the cytoplasm to the nuclei through the nuclear pores. R10p53^{tet}-PNA705 conjugates were constructed by forming a disulfide bond between unique cysteine thiol groups present in the p53 peptide and the PNA705 (Table 1) (*17*). A monomeric PNA705 conjugated to a R10p53^{mono} peptide was also synthesized to serve as a control. The monomeric form of the p53 tet domain was generated by introducing a single mutation (L344P) within its sequence: a modification that is known to block tetramer formation (*16*). Both conjugates were purified by reverse-phase HPLC and characterized by MALDI-TOF mass spectral analysis. The oligomerization state of each peptide was confirmed following glutaraldehyde cross-linking experiments with only the tetrameric peptide R10p53^{tet} giving rise to a characteristic ladder of peptide oligomers on SDS PAGE (*18*) (Figure 1). The sequences of the PNA conjugates are presented in Table 1. Light scattering experiments in aqueous solution for the R10p53^{tet}-PNA705 conjugate suggested some level of aggregation, whereas no such signal was observed for the R10p53^{mono}-PNA705 conjugate (data not shown). The exposure of cells to
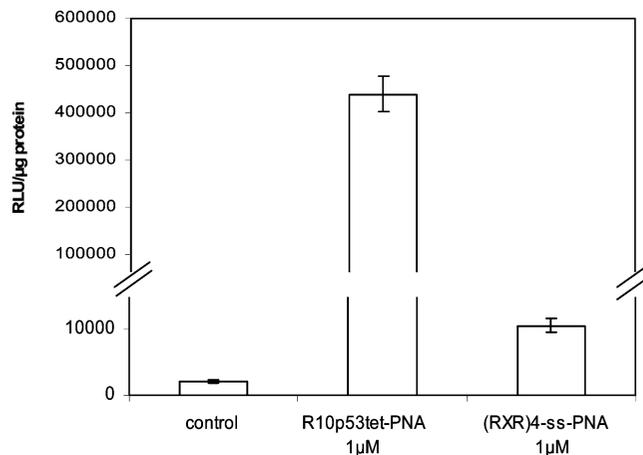

Figure 2. Comparison of R10p53^{tet}-PNA705 with (RAhxR)$_4$-PNA705 in the luciferase assay. Hela pLuc 705 cells were incubated for 4 h with either R10p53^{tet}-PNA705 or (RAhxR)$_4$ PNA705 conjugate at the concentration of 1 μM. After treatment, cells were washed twice with 500 μL PBS, and incubation was continued for 20 h in the presence of complete medium (10% FBS plus DMEM). Luciferase expression was measured 20 h later and was expressed as RLU/μg protein. The control histogram bar represents cells untreated with peptide−PNA conjugates. Each histogram bar represents the averaged RLU/μg protein value with its associated standard deviation derived from experiments performed in triplicate.

these 10R-p53 peptides did not lead to cell toxicity even at concentrations of up to 25 μM (the highest concentration tested; ref 16).

R10p53^{tet}-PNA Is Very Effective at Correcting a Defective Luciferase Reporter Gene Located Inside Cells. Our first objective was to establish if the construct R10p53^{tet}-PNA705 CPP could enter HeLa pLuc705 cells and perform the splicing redirection function expected of the conjugated steric-block PNA705 oligomer leading to the expression of active luciferase (*2*). This construct was evaluated and compared to the PNA705 conjugate with the cationic CPP (RXR)$_4$ (data not shown). The conjugate was prepared in OptiMEM medium to avoid technical issues arising from the absorption or proteolytic degradation of CPP peptides in serum. Specifically, the presence of serum has been shown by us and others to generally reduce the in vitro efficiency of CPP conjugates (*5, 6, 19*), an effect that does not correlate with their in vivo performance. For instance, (RAhxR)$_4$ PMO conjugates performed poorly in vitro when prepared in serum-containing medium but have been used successfully in vivo in a murine model of Duchenne muscular dystrophy (*9*).

As presented in Figure 2, the treatment of HeLa pLuc705 cells with R10p53^{tet}-PNA705 at 1 μM concentration in the absence of any transfection agent gave rise to an approximately 45-fold higher increase in luciferase signal when compared to the (RXR)$_4$-PNA705 conjugate. In order to monitor whether the increased efficiency of R10p53^{tet}-PNA was due to peptide-based tetramerization, R10p53^{tet}-PNA705 was also compared to its monomeric R10p53^{mono}-PNA counterpart in a dose−response experiment. As expected, the tetrameric form was 10-fold more active in the redirection of luciferase splicing than its monomeric form at nanomolar concentrations (Figure 3A,B). Both peptide conjugates were soluble in the transfection media (OptiMEM), and no signs of toxicity were observed under the tested conditions, as assessed in terms of cell viability and protein levels (data not shown). Using the same experimental samples, it was also demonstrated that the cellular delivery of R10p53^{tet}-PNA705 and R10p53^{mono}-PNA705 constructs at submicromolar concentrations into HeLa pLuc705 cells resulted in

A

B

C

← **268 bp aberrant**

← **142 bp correctly spliced**
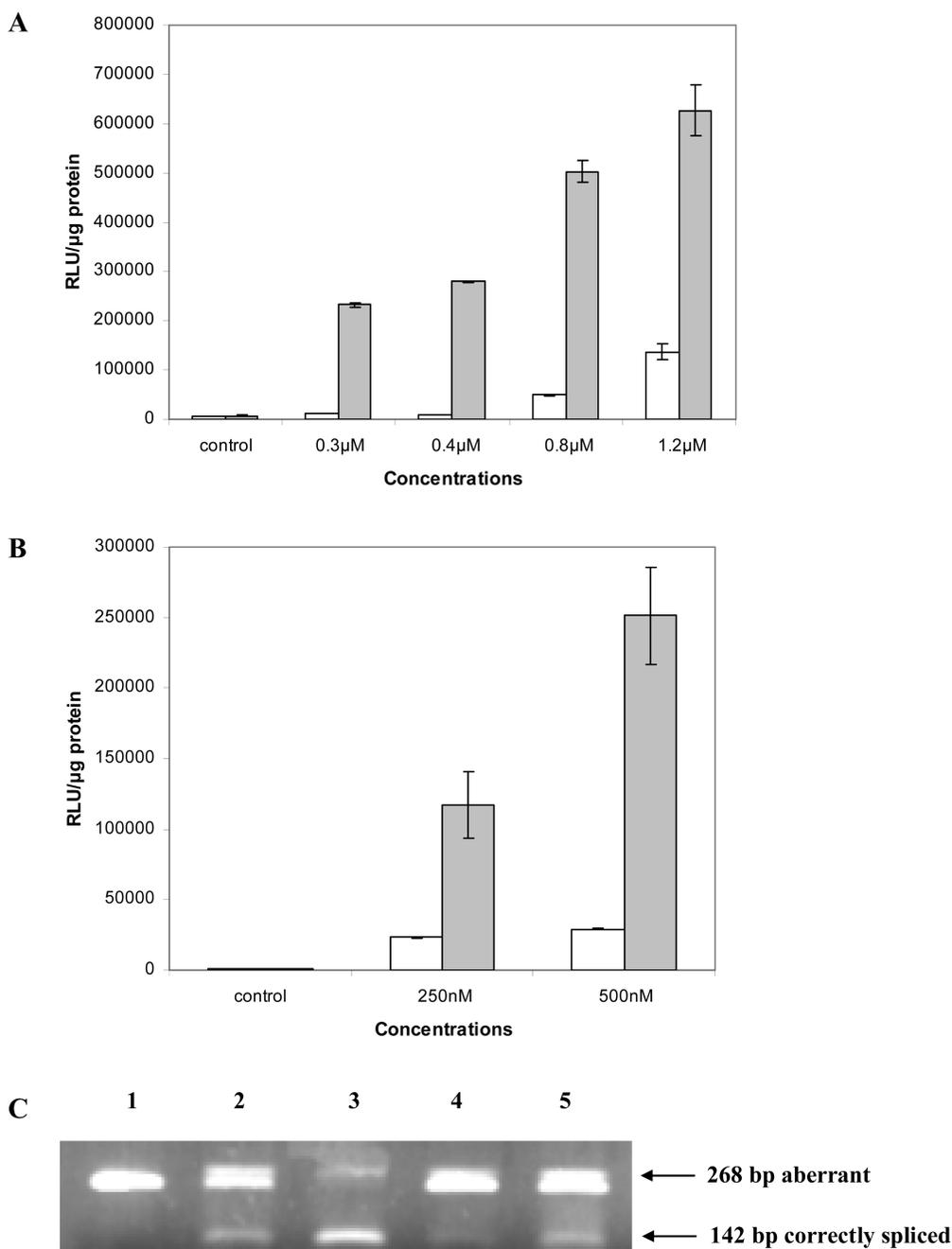
Figure 3. Effect of peptide−PNA concentration on cellular gene correction event. Panels A and B. Dependency of cellular luciferase activity on extracellular peptide−PNA concentration as derived from two separate experiments. HeLa pLuc 705 cells were incubated for 1 h in medium containing R10p53[tet]-PNA705 (gray bars) or R10p53[mono]-PNA705 (white bars) conjugates at the indicated concentrations. Luciferase expression was measured 20 h later and expressed as RLU/μg protein. Each histogram bar represents the averaged RLU/μg protein value with its associated standard deviation derived from experiments performed in triplicate. Panel C. RT-PCR detection of correctly spliced transcripts in HeLa pLuc 705 cells at nanomolar concentrations of R10p53-PNA constructs. Lane 1, Nontreated cells (control); Lane 2, R10p53[tet]-PNA705 250 nM; Lane 3, R10p53[tet]-PNA705 500 nM; Lane 4, R10p53[mono]-PNA705 250 nM; Lane 5, R10p53[mono]-PNA705 500 nM. The RT-PCR experiment was performed with cellular lysates used for generating panel B. The upper band corresponds to the aberrantly spliced luciferase mRNA and the lower band to the correctly spliced mRNA.

the correct splicing of the luciferase transcript at the RNA level (Figure 3C). In brief, treated cells were lysed, and aliquots were processed either for the luciferase luminescence assay or for an RT-PCR assay where the two forms (aberrant and correctly spliced) of luciferase mRNA were amplified. The appearance of the correctly spliced mRNA was dose-dependent and matched the decrease of the aberrantly spliced mRNA. Again, the splicing redirection event was significantly more pronounced for the tetrameric conjugate when compared to its monomeric counterpart.

Mechanism of Cellular Uptake. The mechanism by which cationic CPP−cargo conjugates enter cells is defined by the CPP valency/aggregation state within complexes (*13, 16*) and the concentration of the CPP/cargoes complexes outside cells. At extracellular CPP concentrations in the 5−100 μM range, cationic CPPs can enter cells via both endocytic and membrane-active mechanisms, which explains the co-observation of both energy-dependent endocytotic and energy-independent entry pathway(s) (*20*). However, the practicality of using CPPs in vivo as delivery vectors would favor their
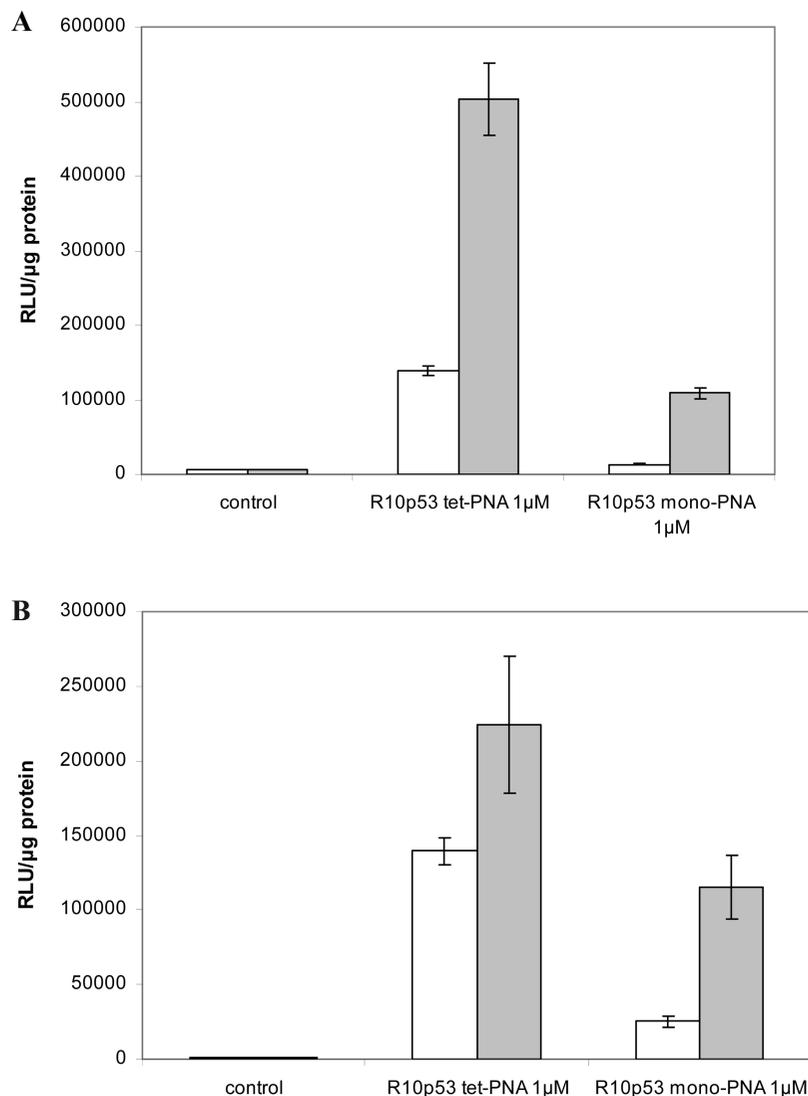
Figure 4. Mechanism of peptide−PNA internalization. Panel A: R10p53^{tet}-PNA and R10p53^{mono}-PNA conjugates are internalized by an energy-dependent mechanism. The splicing correction assay was used to assess the effect of temperature (energy dependency) on peptide−PNA delivery into cells. HeLa pLuc 705 cells were preincubated for 30 min at 4 °C (white bars) or at 37 °C (gray bars) and subsequently exposed to R10p53-PNA conjugates (1 μM) for 1 h under the same conditions. Panel B: Effect of chloroquine on the cytosolic delivery of peptide−PNA constructs leading to luciferase gene correction in HeLa pLuc 705 cells. Cells were incubated for 1 h with either R10p53^{tet} -PNA705 or R10p53^{mono}-PNA705 conjugates (1 μM) in the absence (white bars) or presence (gray bars) of 100 μM chloroquine. Luciferase expression was measured 23 h later and expressed as RLU/μg protein. Each histogram bar represents the averaged RLU/μg protein value with its associated standard deviation derived from experiments performed in triplicate.

use at low micromolar to submicromolar concentrations where their membrane active properties are not observed. Thus, a comparison of the mechanism of cell entry of the tetrameric and monomeric R10p53-PNA705 constructs seemed worthwhile. Therefore, cells were first preincubated at 37 °C or at 4 °C (i.e., at a temperature that prevents any form of endocytosis) before being treated with the conjugates under the same conditions for 1 h. The results (Figure 4A) show a much-reduced splicing redirection activity (as measured by the level of luciferase activity) at low temperature for both monomeric and tetrameric constructs, which suggests an endocytotic mechanism of internalization occurring at a 1 μM concentration.

Since endosomal sequestration remains the principal limitation for the cellular delivery of ONs conjugated to CPPs that pass through the endocytotic route, we incubated cells with each form of R10p53-PNA705 in the presence or absence of chloroquine, a well-known endosomolytic agent (*21, 22*). The splicing redirection efficiency of the PNA conjugate was found to be significantly enhanced (7-fold) in relation to the monomeric

conjugate (Figure 4B), which supports the model that entrapment in endocytic vesicles is a limiting step in the cytoplasmic and nuclear release of such conjugates. Interestingly, chloroquine treatment was found to have a much smaller effect on splicing redirection in the case of R10p53^{tet}-PNA705.

Effect of Saponin Treatment. To circumvent the endocytotic pathway, cells were treated under mild conditions with saponin (20 μg/mL), a detergent which transiently permeabilizes the plasma membrane without damaging cells (*23*). Coincubation of R10p-53^{mono}-PNA705 conjugate with saponin gave the expected substantial augmentation of the splicing redirection activity (Figure 5) consistent with other cationic CPP−PNAs previously tested (*7*). However, the observed luciferase expression level remained lower than the value obtained for the tetrameric conjugate without permeabilization. The effect of saponin treatment on the cellular delivery of R10p53^{tet}-PNA705 led to a lower splicing redirection activity comparable to splicing levels observed for the monomeric conjugate. One possible explanation for this result is that the tetrameric conjugate dissociates when coincubated with detergent (loss of valency), behaving the same way as the monomeric
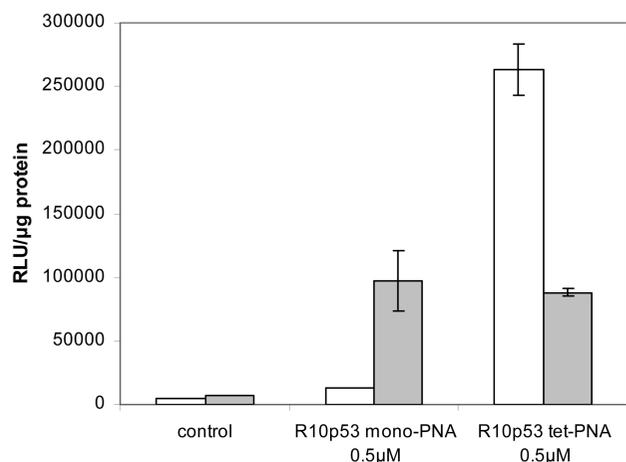
Figure 5. Effect of saponin on delivering peptide−PNA constructs into HeLa pLuc 705 cells. HeLa pLuc705 cells were coincubated with either R10p53^{tet} -PNA705 or R10p53^{mono}-PNA705 conjugates (0.5 μM) in the absence (gray bars) or presence (white bars) of saponin for 30 min. The expression of properly corrected luciferase gene product in HeLa pLuc705 cells was measured as previously described. Each histogram bar represents the averaged RLU/μg protein value with its associated standard deviation derived from experiments performed in triplicate.

conjugate. As shown in Figure 1 (lane C), detergents such as SDS do dissociate the tetramer.

DISCUSSION

Previous work has established that CPP oligomerization through the construction of peptide dendrimers can significantly improve cellular uptake and cytoplasmic delivery of arginine-rich CPPs. The potential of displaying multiple CPPs and their cargoes in the context of the p53 tetramerization domain was evaluated here using a well-characterized splicing redirection assay. The R10p53^{tet}-PNA construct was approximately 45 times more efficient than (RXR)$_4$PNA (Figure 2) and even more active than the Pip2b-PNA construct (ref 9 and data not shown). These results are important, since the Pip series represented until now the most efficient cationic CPP-based PNA delivery vectors.

In order to verify whether the increased efficiency of the R10p53^{tet}-PNA was effectively due to its tetrameric configuration, a monomeric version (R10p53^{mono}-PNA) was engineered through the replacement of leucine 344 by a proline residue, a mutation known to prevent the tetramerization of p53 peptide. Splicing redirection was reduced by a factor of about 10 in keeping with the reduced transfection of a plasmid DNA previously reported by Kawamura and her co-workers (16). However, notable differences between the constructs used in these studies should be pointed out. First, the R10p53^{tet}- and R10p53^{mono}- conjugates used in this study do not include a nuclear localization signal (NLS), in contrast to the NLS-10R-P53^{tet} constructs used to condense and transfect luciferase and β-galactosidase reporter plasmids. Also, the number of NLS-10R-p53^{tet} or NLS-10R-p53^{mono} peptides complexed to a single plasmid was not defined in our previous study (16). Specifically, the CPP-mediated delivery of DNA plasmids requires that cationic CPPs fulfill more than one role: first, by acting to neutralize the anionic character of plasmid DNA and, second, by condensing the resulting complexes into particles that retain the capacity of CPPs to cause cellular import. By contrast, the role of the present 10Rp53 peptides is limited to the cellular internalization and trafficking of an uncharged PNA cargo. Specifically, the single 18-base-long PNA705 was chemically conjugated to the CPP moiety such that the resulting monomers and tetramers obtained are simple, well-defined structures. Al-

together, the present study provides a more direct evaluation of the potential of oligomerization on the nuclear delivery of a cargo.

As highlighted in Figures 2−5, the tetrameric R10p53^{tet}-PNA705 construct represents by far the most effective peptide-PNA705 construct to date in terms of correcting the genetic defect present in HeLa pLuc705 cells. This construct was able to deliver an effective dose of the PNA705 peptide nucleic acid to the cytosol of these cells when present outside HeLa pLuc705 cells at nanomolar concentrations. Somewhat unexpectedly, the R10p53^{mono}-PNA construct remained slightly more active than the (RXR)$_4$PNA conjugate. Clues as to why both R10p53-PNAs are more effective in delivering PNA705 to cells than the (RXR)$_4$PNA conjugate may be linked to two parameters. First, the spacial presentation of CPPs on a p53^{tet} scaffold (branched display where CPPs are equivalently presented) is not identical to that of the (RXR)$_4$PNA conjugate (single CPP consisting of a linear sequence of short internal diarginyl-containing peptide motifs). Second, the p53 constructs possess a higher arginine content (4 × 10 Arg; p53^{tet} scaffold and 10 Arg for the monomeric form) than in the case of the (RXR)4-ss-PNA (4 × 2 Arg) construct. Finally, the presence of the hexahistidine tag in the p53 constructs may also be consequential.

Further studies will be required to identify what features of the p53 peptide and (His)$_6$ domains (see Table 1 for the complete sequence) have a positive impact on PNA delivery.

The mechanism by which CPP−cargo conjugates enter cells remains in part dependent on the steady-state levels of CPP concentration outside cells. Mechanisms involving a direct energy-independent translocation (20, 23) as well as various endocytotic pathways (24−27) have been proposed. Dominance of one or another internalization pathways appears to be linked to the concentration of CPP-conjugates experienced by cells with high local (membrane-bound) concentration of CPP-conjugates (high micromolar range) favoring the aggregation and membrane-active properties of cationic peptides allowing for their direct cell translocation, whereas low CPP concentrations lead to internalization via proteoglycan binding and to endocytic pathways (28, 29). As an in vivo drug delivery strategy, CPP concentrations needed to achieve energy-independent translocation are too high (>10 μM) to be effective and may result in cell cytotoxicity.

Internalization of both the tetramer and the monomer R10p53-PNA constructs is energy dependent as previously demonstrated for R10p53 peptides (16) and in our functional assay when R10p53 peptides deliver their PNA705 cargo. Specifically, the exposure of HeLa pLuc705 cells to low temperature reduces the expression of functional luciferase driven by the presence of either R10p53 constructs in the medium (Figure 4A). These findings are in accordance with previous work reporting a clathrin-mediated endocytotic pathway of cell uptake for fluorescein-tagged 10R-p53^{tet} peptides (16).

Taken together, these observations do not point to differences in the cellular entry mechanism as an explanation for the increased efficiency of R10p53^{tet}-PNA as compared to its monomeric analogue or to (RXR)$_4$PNA. A significant fraction of R10p53 peptides remains trapped in endosomes. As expected, chloroquine treatment, which is known to promote endosomal release of entrapped CPP−cargo conjugates (30), indeed causes a significantly more pronounced increase in splicing correction for R10p53^{mono}-PNA compared to R10p53^{tet}-PNA (Figure 4B). Whether this increased ability to escape endocytic vesicles is the only determinant of the increased splice redirecting activity of R10p53^{tet}-PNA as compared to the monomeric form cannot be ascertained on this basis. The presence of chloroquine is thus not essential for cellular delivery using the R10p53^{tet}-PNA

construct. Interestingly, (RAhxR)$_4$ PMO conjugates have been used in vivo (in the absence of the lysosomotropic amine agent chloroquine) and were able to promote exon skipping in the *mdx* mouse model of Duchenne muscular dystrophy (*9*). The constructs used in the present study are more efficient in vitro than these (RAhxR)$_4$ PMO constructs when compared in the same assay in the absence of chloroquine. Thus, we expect that they might be more efficient in vivo in the absence of chloroquine.

We thus attempted to deliberately bypass endocytosis by submitting cells to a brief saponin treatment under mild conditions, known to transiently permeabilize the plasma membrane with minimal alteration of cell physiology (*23*). As expected and in line with previous data from our group for other CPP−PMO/PNA conjugates (*7*), splicing correction by R10p53^{mono}-PNA was increased in saponin-treated cells but did not reach the efficiency achieved by R10p53^{tet}-PNA in untreated cells. One of the many possible explanations could be that the more bulky R10p53^{tet}-PNA construct more efficiently masks the cryptic splice site and reorients the splicing machinery. Unexpectedly, splicing redirection was less efficient in saponin-treated cells for the R10p53^{tet}-PNA construct. It might be due to a conversion of the tetrameric form into the monomeric form upon saponin treatment.

Altogether, our results confirm the potential of CPP oligomerization as a strategy to enhance the delivery of conjugated cargoes into cells. Specifically, the cellular delivery and splicing activity of PNA705 observed at nanomolar concentrations for the tetrameric R10p53-PNA construct is remarkable when compared to all other CPP strategies tested to date. This study provides a proof-of-concept for exploiting multivalent CPP strategies in the context of in vivo applications. Future work by our group will include the grafting of CPPs and cargoes onto simpler synthetic dendrimeric scaffolds.

LITERATURE CITED

(1) Rayburn, R. E., and Zhang, R. (2008) Antisense, RNAi, and gene silencing strategies for therapy: mission possible or impossible? *Drug Discovery Today 13*, 513–521.

(2) Kang, S. H., Cho, M. J., and Kole, R. (1998) Up-regulation of luciferase gene expression with antisense oligonucleotides: implications and applications in functional assay development. *Biochemistry 37*, 6235–6239.

(3) Abes, R., Arzumanov, A. A., Moulton, H. M., Abes, S., Ivanova, G. D., Iversen, P. L., Gait, M.J., and Lebleu, B. (2007) Cell-penetrating-peptide-based delivery of oligonucleotides: an overview. *Biochem. Soc. Trans. 35*, 775–779.

(4) El Andaloussi, S., Guterstam, P., and Langel, U. (2007) Assessing the delivery efficacy and internalization route of cell-penetrating peptides. *Nat. Protoc. 2*, 2043–2047.

(5) Wu, R. P., Youngblood, D. S., Hassinger, J. N., Lovejoy, C. E., Nelson, M. H., Iversen, P. L., and Moulton, H. M. (2007) Cell-penetrating peptides as transporters for morpholino oligomers: effects of amino acid composition on intracellular delivery and cytotoxicity. *Nucleic Acids Res. 35*, 5182–5191.

(6) Koppelhus, U., Shiraishi, T., Zachar, V., Pankratova, S., and Nielsen, P. E. (2008) Improved cellular activity of antisense peptide nucleic acids by conjugation to a cationic peptide-lipid (CatLip) domain. *Bioconjugate Chem. 19*, 1526–1534.

(7) Abes, R., Moulton, H. M., Clair, P., Yang, S. T., Abes, S., Melikov, K., Prevot, P., Youngblood, D. S., Iversen, P. L., Chernomordik, L. V., and Lebleu, B. (2008) Delivery of steric block morpholino oligomers by (R-X-R)4 peptides: structure-activity studies. *Nucleic Acids Res. 36*, 6343–6354.

(8) Abes, S., Turner, J. J., Ivanova, G. D., Owen, D., Williams, D., Arzumanov, A., Clair, P., Gait, M. J., and Lebleu, B. (2007) Efficient splicing correction by PNA conjugation to an R6-Penetratin delivery peptide. *Nucleic Acids Res. 35*, 4495–4502.

(9) Ivanova, G. D., Arzumanov, A., Abes, R., Yin, H., Wood, M. J., Lebleu, B., and Gait, M. J. (2008) Improved cell-penetrating peptide-PNA conjugates for splicing redirection in HeLa cells and exon skipping in mdx mouse muscle. *Nucleic Acids Res. 36*, 6418–6428.

(10) Yin, H., Lu, Q., and Wood, M. (2008) Effective exon skipping and restoration of dystrophin expression by peptide nucleic acid antisense oligonucleotides in mdx mice. *Mol. Ther. 16*, 38–45.

(11) Yin, H., Moulton, H. M., Seow, Y., Boyd, C., Boutilier, J., Iverson, P., and Wood, M. J. (2008) Cell-penetrating peptide-conjugated antisense oligonucleotides restore systemic muscle and cardiac dystrophin expression and function. *Hum. Mol. Genet. 17*, 3909–3918.

(12) Sheldon, K., Liu, D., Ferguson, J., and Gariépy, J. (1995) Loligomers: design of de novo peptide-based intracellular vehicles. *Proc. Natl. Acad. Sci. U.S.A. 92*, 2056–2060.

(13) Sung, M., Poon, G. M., and Gariépy, J. (2006) The importance of valency in enhancing the import and cell routing potential of protein transduction domain-containing molecules. *Biochim. Biophys. Acta, Biomembr. 1758*, 355–363.

(14) Singh, D., Bisland, S. K., Kawamura, K., and Gariépy, J. (1999) Peptide-based intracellular shuttle able to facilitate gene transfer in mammalian cells. *Bioconjugate Chem. 10*, 745–754.

(15) Bisland, S. K., Singh, D., and Gariépy, J. (1999) Potentiation of chlorin e6 photodynamic activity in vitro with peptide-based intracellular vehicles. *Bioconjugate Chem. 10*, 982–992.

(16) Kawamura, K. S., Sung, M., Bolewska-Pedyczak, E., and Gariépy, J. (2006) Probing the impact of valency on the routing of arginine-rich peptides into eukaryotic cells. *Biochemistry 45*, 1116–1127.

(17) Turner, J. J., Ivanova, G. D., Verbeure, B., Williams, D., Arzumanov, A. A., Abes, S., Lebleu, B., and Gait, M. J. (2005) Cell-penetrating peptide conjugates of peptide nucleic acids (PNA) as inhibitors of HIV-1 Tat-dependent trans-activation in cells. *Nucleic Acids Res. 33*, 6837–6849.

(18) Poon, G. M., Brokx, R. D., Sung, M., and Gariépy, J. (2007) Tandem dimerization of the human p53 tetramerization domain stabilizes a primary dimer intermediate and dramatically enhances its oligomeric stability. *J. Mol. Biol. 365*, 1217–1231.

(19) Abes, S., Williams, D., Prevot, P., Thierry, A., Gait, M. J., and Lebleu, B. (2006) Endosome trapping limits the efficiency of splicing correction by PNA-oligolysine conjugates. *J. Controlled Release 110*, 595–604.

(20) Ter-Avetisyan, G., Tunnemann, G., Nowak, D., Nitschke, M., Herrmann, A., Drab, M., and Cardoso, M. C. (2009) Cell entry of arginine-rich peptides is independent of endocytosis. *J. Biol. Chem. 284*, 3370–3378.

(21) Ciftci, K., and Levy, R. J. (2001) Enhanced plasmid DNA transfection with lysosomotropic agents in cultured fibroblasts. *Int. J. Pharm. 218*, 81–92.

(22) Abes, S., Williams, D., Prevot, P., Thierry, A., Gait, M. J., and Lebleu, B. (2006) Endosome trapping limits the efficiency of splicing correction by PNA-oligolysine conjugates. *J. Controlled Release 110*, 595–604.

(23) Hudder, A., Nathanson, L., and Deutscher, M. P. (2003) Organization of mammalian cytoplasm. *Mol. Cell. Biol. 23*, 9318–9326.

(24) Duchardt, F., Fotin-Mleczek, M., Schwarz, H., Fischer, R., and Brock, R. (2007) A comprehensive model for the cellular

uptake of cationic cell-penetrating peptides. *Traffic (Oxford, U.K.) 8*, 848–866.

(25) Richard, J. P., Melikov, K., Vives, E., Ramos, C., Verbeure, B., Gait, M. J., Chernomordik, L. V., and Lebleu, B. (2003) Cell-penetrating peptides. A reevaluation of the mechanism of cellular uptake. *J. Biol. Chem. 278*, 585–590.

(26) Richard, J. P., Melikov, K., Brooks, H., Prevot, P., Lebleu, B., and Chernomordik, L. V. (2005) Cellular uptake of unconjugated TAT peptide involves clathrin-dependent endocytosis and heparan sulfate receptors. *J. Biol. Chem. 280*, 15300–15306.

(27) Kaplan, I. M., Wadia, J. S., and Dowdy, S. F. (2005) Cationic TAT peptide transduction domain enters cells by macropinocytosis. *J. Controlled Release 102*, 247–253.

(28) Fretz, M. M., Penning, N. A., Al-Taei, S., Futaki, S., Takeuchi, T., Nakase, I., Storm, G., and Jones, A. T. (2007) Temperature-, concentration- and cholesterol-dependent translocation of L- and D-octa-arginine across the plasma and nuclear membrane of CD34+ leukaemia cells. *Biochem. J. 403*, 335–342.

(29) Poon, G. M., and Gariépy, J. (2007) Cell-surface proteoglycans as molecular portals for cationic peptide and polymer entry into cells. *Biochem. Soc. Trans. 35*, 788–793.

(30) Abes, S., Moulton, H. M., Clair, P., Prevot, P., Youngblood, D. S., Wu, R. P., Iversen, P. L., and Lebleu, B. (2006) Vectorization of morpholino oligomers by the (R-Ahx-R)4 peptide allows efficient splicing correction in the absence of endosomolytic agents. *J. Controlled Release 116*, 304–313.